Experimental measurement of resonance islands induced by rf voltage modulation

D. Li,[1] M. Ball,[1] B. Brabson,[1] J. Budnick,[1] D. D. Caussyn,[1] A. W. Chao,[2]
J. Collins,[1] V. Derenchuk,[1] S. Dutt,[2] G. East,[1] M. Ellison,[1] D. Friesel,[1] B.
Hamilton,[1] H. Huang,[1] W. P. Jones,[1] S. Y. Lee,[1] M. G. Minty,[3] S. Nagaitsev,[1]
K. Y. Ng,[4] X. Pei,[6] T. Sloan,[1] M. Syphers,[2] L. Teng,[5] Y. Wang,[1] Y.T. Yan,[2]
and P.L. Zhang[2]

[1]*Indiana University Cyclotron Facility, Indiana University, Bloomington, Indiana 47405*
[2]*Superconducting Supercollider Laboratory, 2550 Beckleymeade Avenue, Dallas, Texas 75237-3946*
[3]*Stanford Linear Accelerator Center, MS26, Box 4349, Stanford, California 94309*
[4]*Fermilab, P.O. Box 500, Batavia, Illinois 60510*
[5]*Advanced Photon Source, Argonne National Laboratory, 9700 South Cass Avenue, Argonne, Illinois 60439*
[6]*Brookhaven National Laboratory, Upton, New York 11973*
(Received 2 June 1993)

Synchrotron motion with an external rf voltage modulation was studied experimentally. Beam particles, in the presence of electron cooling, were observed to damp to the basins of resonance islands, which were produced by the parametric resonance due to rf voltage modulation. The measured phase amplitudes of the centers of these resonance islands were found to agree well with theory.

PACS number(s): 41.85.−p, 05.45.+b, 29.20.Dh

The rf voltage modulation is one of the important beam dynamics topics in accelerator physics. Problems related to rf voltage modulation include rf noise and power supply ripple [1], parametric feedback for multibunch instabilities [2], and the possibility of using rf voltage modulation for the superslow extraction in future high-energy colliders [3]. Thus careful theoretical and experimental studies of synchrotron motion with rf voltage modulation provide understanding of these beam dynamics issues. This paper reports experimental results of beam dynamics studies with voltage modulation at the Indiana University Cyclotron Facility (IUCF) Cooler Ring.

The experiment started with a single bunch of about 5×10^8 protons with kinetic energy of 45 MeV. The cycle time was 10 s, where the injected beam was electron-cooled for about 3 s, producing a full width at half maximum bunch length of about 9 m (or 100 ns) depending on the rf voltage. The low frequency rf system used in the experiment was operating at the harmonic number $h = 1$ with frequency 1.031 68 MHz. The experimental hardware has been reported in previous publications [4, 5].

The voltage control feedback of the IUCF Cooler rf system works as follows. The cavity rf voltage is picked up and rectified into dc via synchronous detection. The rectified dc signal is compared to a preset voltage. The resulting error goes through a nearly ideal integrator that has very high dc gain. The integrated signal is then used to control an attenuator regulating the level of the rf signal being fed to the rf amplifiers. Because of the electrical inertia of the cavity, a phase delay in the signal also occurs. Near the resonance of the cavity, this phase delay can reach a maximum of 90°. In addition to the 90° phase delay of the integrator, the cavity phase delay could cause a total of a 180° phase delay of the feedback

loop, thereby producing a positive feedback. To prevent this adverse phase condition, a signal proportional to the phase error, called phase lead compensation, is added to the attenuator control. The amplitude modulation is summed with the reference to be compared to the cavity sample signal. The modulation causes a change in the error voltage sensed by the control loop and results in modulation of the attenuator around a given cavity voltage preset. The maximum rate of modulation is limited by the loop response time of about 10 kHz. The modulation rates in our experiments are well within this limit. The modulation amplitude was measured and calibrated.

With rf voltage modulation, the synchrotron mapping equations are given by

$$\phi_{n+1} = \phi_n + 2\pi\nu_s\delta_n,$$

$$\delta_{n+1} = \delta_n - 2\pi\nu_s[1 + \epsilon\sin(\nu_m\theta_{n+1} + \chi)]\sin\phi_{n+1} - 2\pi\frac{2\alpha}{\omega_0}\delta_n,$$

where $(\phi, \ \delta = \frac{h\eta}{\nu_s}\frac{\Delta p}{p})$ are conjugate phase space coordinates for the phase and the normalized momentum spread, respectively; η is the phase slip factor; $\nu_s = \sqrt{\frac{h|\eta|eV}{2\pi\beta^2 E}}$ is the synchrotron tune at zero amplitude; the orbital angle θ is used as the time variable; ϵ is the percentage rf voltage modulation strength; χ is a phase factor; $\omega_0 = 2\pi f_0$ is the angular revolution frequency; ν_m is the modulation tune; and α is the phase space damping factor for electron cooling at the IUCF Cooler Ring, which was measured to be about 2.5 s^{-1} $\ll \omega_0\nu_s$. In this experiment, the synchrotron frequency is about $f_s = f_0\nu_s = 263$ Hz, $\epsilon = 0.05$, and $\eta = -0.86$.

Neglecting the damping term, the synchrotron equations of motion can be derived from the following Hamiltonian:

$$H = \tfrac{1}{2}\nu_s\delta^2 + \nu_s[1 + \epsilon\sin(\nu_m\theta + \chi)][1 - \cos\phi].$$

In order to see the resonance structure induced by the external modulation, we transform the phase space coordinates, (ϕ,δ), into the action-angle variables (J,ψ) where the action variable is given by $J = \frac{1}{2\pi}\oint \delta d\phi$. When the action is small, i.e., $J \leq 2$, the action-angle variables can be obtained approximately by the canonical transformation using the generating function, $F_1(\phi,\psi) = -\frac{\phi^2}{2}\tan\psi$, with $\phi = \sqrt{2J}\cos\psi$, $\delta = -\sqrt{2J}\sin\psi$. The new Hamiltonian can be approximated by (with $\chi = 0$ for simplicity)

$$H \approx \nu_s J - \frac{\nu_s}{16}J^2 + \nu_s\epsilon\sin(\nu_m\theta)[1 - J_0(\sqrt{2J})]$$
$$+ \sum_{k=1}^{\infty}(\Delta H_{2k}^{(+)} + \Delta H_{2k}^{(-)}), \qquad (1)$$

where

$$\Delta H_{2k}^{(\pm)} = \nu_s\epsilon(-1)^{k+1}J_{2k}(\sqrt{2J})\sin(\nu_m\theta \pm 2k\psi),$$
$$k = 1,2,\ldots, \quad (2)$$

and J_n are Bessel functions of the order n. The sinusoidal modulation of the rf cavity voltage produces oscillating terms which are in phase or out of phase with the synchrotron oscillations. When the modulation frequency equals an even harmonic of the synchrotron frequency, i.e., $\nu_m \approx 2k\nu_s, k = 1,2,\ldots, \Delta H_{2k}^{(-)}$ becomes important.

As an example, we consider the resonance near the second harmonic, i.e., $k = 1$. The island structure is revealed by transforming the coordinate system to the resonance precessing frame using the generating function, $F_2(\psi,\tilde{J}) = (\psi - \frac{\nu_m}{2}\theta - \frac{3\pi}{4})\tilde{J}$, with the coordinate transformation, $\tilde{\psi} = \psi - \frac{\nu_m}{2}\theta - \frac{3\pi}{4}$ and $J = \tilde{J}$. In terms of the new variables, the Hamiltonian becomes

$$\tilde{H} = \left(\nu_s - \frac{\nu_m}{2}\right)\tilde{J} - \frac{\nu_s}{16}\tilde{J}^2 + \frac{\nu_s}{4}\epsilon\tilde{J}\cos 2\tilde{\psi}$$
$$+ \Delta H(\tilde{J},\tilde{\psi},\theta),$$

where the time dependent part of the perturbing Hamiltonian, $\Delta H(\tilde{J},\tilde{\psi},\theta)$, is oscillating at the frequencies of $\nu_m, 2\nu_m, \ldots$.

Because of the resonance (or stationary phase) condition, i.e., $\frac{d\tilde{\psi}}{d\theta} \approx 0$, the time independent term of the Hamiltonian contributes coherently, while the time dependent terms contribute incoherently to equations of motion. The particle trajectories in phase space can then be described by tori of the time-averaged Hamiltonian,

$$\langle\tilde{H}\rangle = \left(\nu_s - \frac{\nu_m}{2}\right)\tilde{J} - \frac{\nu_s}{16}\tilde{J}^2 + \frac{\nu_s}{4}\epsilon\tilde{J}\cos 2\tilde{\psi}, \qquad (3)$$

which is an invariant. For simplicity, we drop the tilde notations. The trajectories of the particle motion, obeying Hamilton's equations of motion, trace out tori of the Hamiltonian flow. The stable fixed points (SFP's) are located at

$$J_{\text{SFP}} = 8\left(1 - \frac{\nu_m}{2\nu_s}\right) + 2\epsilon, \qquad (4)$$

for $\psi = 0$ and π with $\nu_m \leq 2(1 + \frac{\epsilon}{4})\nu_s$, and the unstable fixed points (UFP's) located at

$$J_{\text{UFP}} = \begin{cases} 8(1 - \frac{\nu_m}{2\nu_s}) - 2\epsilon & \text{if } \nu_m \leq 2\nu_s - \frac{1}{2}\epsilon\nu_s, \\ 0 & \text{if } 2\nu_s - \frac{1}{2}\epsilon\nu_s \leq \nu_m \leq 2\nu_s + \frac{1}{2}\epsilon\nu_s \end{cases} \qquad (5)$$

for $\psi = \frac{\pi}{2}$ and $\frac{3\pi}{2}$. These results can be summarized as follows.

(1) When the modulation tune ν_m is larger than $\nu_1 = (2 + \frac{1}{2}\epsilon)\nu_s$, the origin is a SFP of the Hamiltonian.

(2) When the modulation tune lies between $[\nu_2,\nu_1]$, where $\nu_2 = (2 - \frac{1}{2}\epsilon)\nu_s$, the SFP at the origin bifurcates and the origin becomes unstable [6] shown in the lower part of Fig. 1.

(3) When the modulation tune is lower than ν_2, the UFP at the origin bifurcates due to the nonlinearity shown in the upper part of Fig. 1. The origin is again stable.
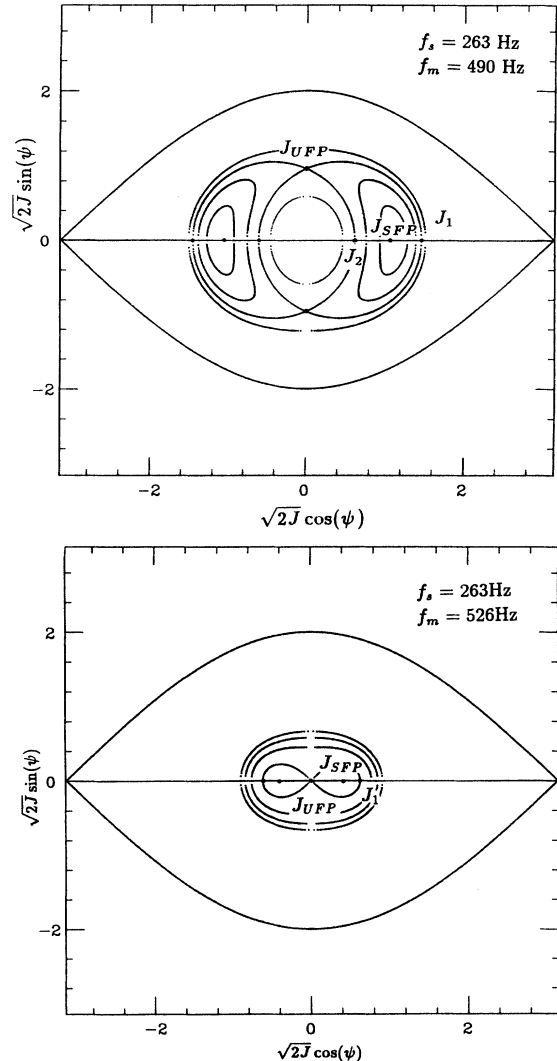
The separatrix, which determines the stability bound-

FIG. 1. The separatrix and tori of the time independent Hamiltonian (3) are plotted and the actions $J_{\text{SFP}}, J_{\text{UFP}}, J_1$, and J_2 are marked.

ary of resonance islands, is the torus passing through UFP's. The intercepts of the separatrix with the phase coordinate at the actions, J_1, J_2 marked in Fig. 1, are useful quantities for the maximum phase oscillation amplitude.

By including a weak damping term, the Hamiltonian flow may be distorted, yet the island structure remains intact provided that the damping coefficient is small. After several damping time periods, $\frac{1}{\alpha}$, particles in phase space are trapped in islands. The exact island that a particle is trapped in depends on the initial particle phase space coordinates [5]. Figure 2 shows the final beam distribution after 5×10^5 revolutions obtained from a numerical tracking of the synchrotron motion with rf voltage modulation using the following parameters: $\epsilon = 0.05$, $f_m = 478$ Hz, $f_s = 262$ Hz, and the damping coefficient $\alpha = 2.5$ s^{-1}. The initial conditions of 192×192 particles were assumed to be uniformly distributed in a rectangular box, $\phi \in [-\pi, \pi]$, $\delta \in [-2, 2]$. In addition to the attractor at the center of the bucket, there are two attractors given by the SFP of Eq. (4). These two beamlets are rotating around the center of the rf bucket with an angular frequency equal to one half of the modulation frequency. The numerical simulation also predicts two more attractors located at the separatrix of the rf bucket, which was populated by those particles located in a patch of initial phase space coordinates outside the separatrix. We also found that the initial phase space coordinates converging towards a specific attractor inside the rf bucket form interwoven nonintersecting spiral rings. The damping path of a single particle, in the resonance precessing frame, follows closely a spiral ring.

Figure 3 shows the accumulated traces of signals from a beam position monitor sum signal on the oscilloscope triggered at the rf frequency. A single trace of the beam bunch was measured using a fast 1×10^9 sample/s scope, HP54510A, to confirm that there were indeed three separate beamlets in the bucket. The phase amplitudes of outer attractors were measured by using an oscilloscope. The actions of the stable fixed points, J_{SFP}, are compared in Fig. 4 with the measured actions of the outer beam-

FIG. 3. The longitudinal beam distribution from a BPM sum signal accumulated over many synchrotron periods as shown on an oscilloscope. Note here that there are three bunches rotating at one half of the modulation frequency about the center of the rf bucket.

lets as a function of the modulation frequency. The data shown with different symbols (circles, crosses, diamonds, and ×'s) were taken at different times but with a nearly identical rf voltage setting. The actions of the UFP, J_{UFP}, and the intercepts of the separatrix with phase axis, J_1, J_2, are also shown in Fig. 4. Experimentally, we found that the action of the outer attractor depended linearly on the modulation frequency. The synchrotron tune was fitted to be about 263 ± 1 Hz during this run. Our experimental result agreed well with the theoretical pre-
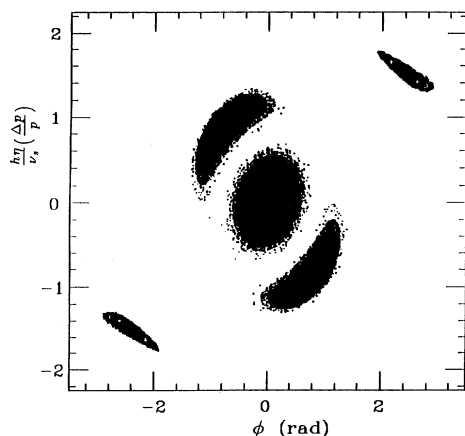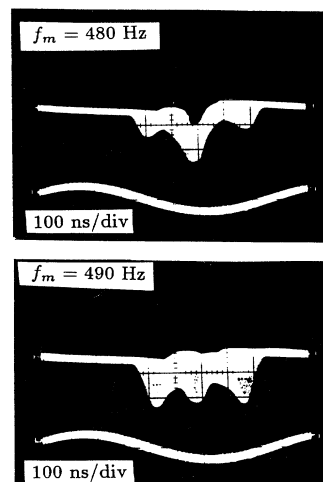

FIG. 2. The beam bunch splitting inside an rf bucket, obtained from numerical simulations with rf voltage modulation and phase space damping.
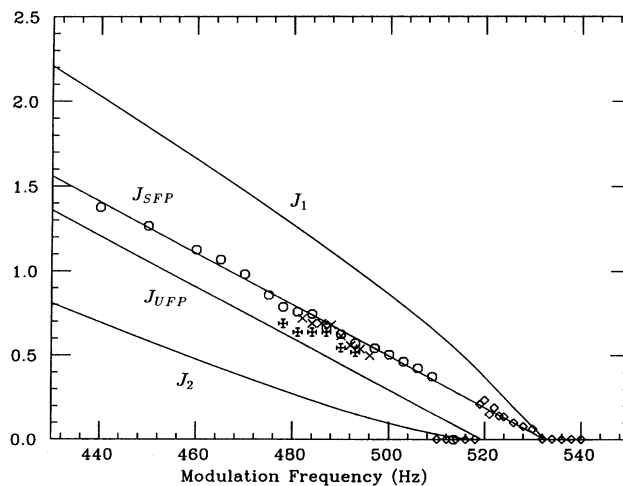

FIG. 4. The measured action of the outer beamlet as a function of the modulation frequency. The different symbols used for the measured data correspond to measurements at different times for an almost identical rf voltage. The solid line of the J_{SFP} obtained from Eq. (4) fits data with $f_s = 263$ Hz. The actions corresponding to the UFP, J_{UFP}, and the intercepts, J_1, J_2, of the separatrix with the phase axis are also shown.

diction except in the region of $f_m \in [510, 520]$ Hz, where we did not observe beam splitting. A possible explanation for this is that the beam was much larger than the island structure, where the stable fixed point was about 100 ns from the center of the bucket. Once f_m reached $2f_s - \frac{1}{2}\epsilon f_s$, where $J_{\text{UFP}} = 0$, the beam was observed to split into only two beamlets. The fact that all islands ceased to exist at $f_m \approx 532$ Hz was also clearly verified from our measurement.

In conclusion, we found that the measured attractor amplitude agreed well with the theoretical prediction for the fixed point of the parametric resonant Hamiltonian. In particular, the parametric excitation at $f_m = 2f_s$ created two resonant islands at the action of $J = 2\epsilon$. The beam bunch with the rf modulation at $2f_s$ becomes the shape of a dumbbell, which spins about the center of the bucket at one-half of the modulation frequency, i.e., the synchrotron frequency. By choosing the modulation phase χ and the modulation strength ϵ properly, the orientation and the size of dumbbells could be adjusted. This mechanism was applied to damp the π-mode coupled bunch instability at the Stanford Linear Accelerator Center (SLAC) damping ring [2]. These parametric resonances in synchrotrons with phase space damping may also be used to control beam dilution, bunch shape rotation, etc.

[1] G. Dôme, CERN Report No. 87-03, p. 370 (1987) (unpublished); S. Krinsky and J.M. Wang, Part. Accel. **12**, 107 (1982).

[2] J.D. Fox, and P. Corredoura, in *Proceedings of the European Particle Accelerator Conference*, edited by H. Henke, H. Homeyer, and Ch. Petit-Jean-Genaz (Springer-Verlag, Heidelberg, 1992), p. 1079.

[3] H.J. Shih and A.M. Taratin, Superconducting Supercollider Laboratory Report No. SSCL-389, 1991 (unpublished); W. Gabella, J. Rosenzweig, R. Kick, and S. Peggs, Fermilab Report No. TM-1783, 1992 (unpublished).

[4] S.Y. Lee *et al.*, Phys. Rev. Lett. **67**, 3768 (1991); D.D. Caussyn *et al.*, Phys. Rev. A **46**, 7942 (1992); M. Ellison *et al.*, Phys. Rev. Lett. **70**, 591 (1993).

[5] M. Syphers *et al.*, Phys. Rev. Lett. **71**, 719 (1993); Y. Wang *et al.* (unpublished).

[6] L.D. Landau and E.M. Lifschitz, *Mechanics*, 3rd. ed. (Pergamon, New York, 1976).